

# RSC Advances



This is an *Accepted Manuscript*, which has been through the Royal Society of Chemistry peer review process and has been accepted for publication.

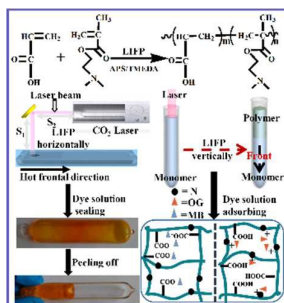
*Accepted Manuscripts* are published online shortly after acceptance, before technical editing, formatting and proof reading. Using this free service, authors can make their results available to the community, in citable form, before we publish the edited article. This *Accepted Manuscript* will be replaced by the edited, formatted and paginated article as soon as this is available.

You can find more information about *Accepted Manuscripts* in the [Information for Authors](#).

Please note that technical editing may introduce minor changes to the text and/or graphics, which may alter content. The journal's standard [Terms & Conditions](#) and the [Ethical guidelines](#) still apply. In no event shall the Royal Society of Chemistry be held responsible for any errors or omissions in this *Accepted Manuscript* or any consequences arising from the use of any information it contains.

# Facile Access to Poly(DMAEMA-co-AA) Hydrogels via Infrared Laser-Ignited Frontal Polymerization and Its Polymerization in Horizontal Direction

Yan Liu, Cai-Feng Wang, Su Chen\*



pH sensitive hydrogels are fabricated via infrared laser-ignited frontal polymerization (LIFP) and its LIFP in horizontal direction towards dye adsorption.

## ARTICLE

# Facile Access to Poly(DMAEMA-*co*-AA) Hydrogels via Infrared Laser-Ignited Frontal Polymerization and Its Polymerization in Horizontal Direction

Cite this: DOI: 10.1039/x0xx00000x

Yan Liu, Cai-Feng Wang, Su Chen\*

Received 00th January 2012,  
Accepted 00th January 2012

DOI: 10.1039/x0xx00000x

www.rsc.org/

A series of poly(DMAEMA-*co*-AA) hydrogels (DMAEMA = dimethylaminoethyl methacrylate, AA = acrylic acid) were quickly produced via infrared laser ignited frontal polymerization (LIFP), and the LIFP in horizontal direction was firstly performed successfully. The dependence of the front velocity and front temperature of LIFP on the molar ratios of AA/DMAEMA and the concentrations of initiator was investigated, along with characterizing swelling capacity and morphology properties of the as-prepared hydrogels. The as-prepared hydrogels are sensitive to pH values ranged from 2 to 12, and their maximum equilibrium swelling ratio could reach 2497 % in pH=7. Moreover, the hydrogels are able to absorb an anionic dye (orange G) and a cationic dye (methylene blue) through electrostatic interaction, offering the potential as dye adsorbents for water purification. On the other hand, LIFP horizontally was employed to seal dyestuff solutions, expanding the scope of LIFP applications on spilled toxic substances without touching the location of the reaction.

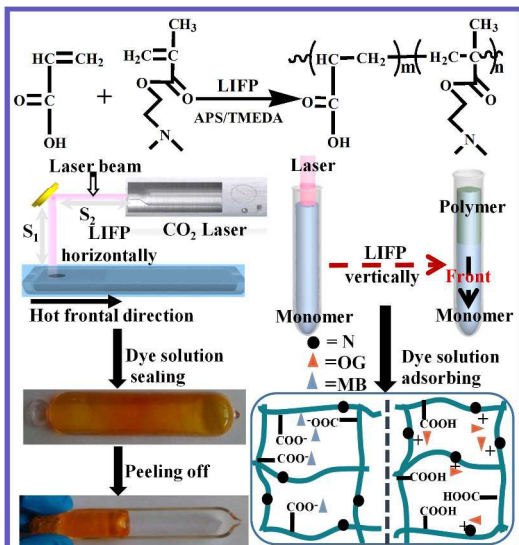
## 1. Introduction

Frontal polymerization<sup>1</sup>(FP) develops the coupling of the Arrhenius kinetics and thermal diffusion of the exothermic polymerization that converts the monomer into polymer via the propagation of a localized reaction zone through the whole system. No further energy is required in the coming reaction process, as long as giving a brief excitation with an external stimulus. Because of its less energy-consuming, time-saving and convenient operation, FP has extracted extensive research interests in the preparation of various polymers, especially in functional hydrogels. In this respect, Washington and Steinbock<sup>2</sup> first fabricated temperature-sensitive poly(N-isopropylacrylamide) hydrogels via FP in 2001. Afterwards, starch-graft-poly(acrylic acid) hydrogels<sup>3,4</sup>, porous polyacrylamide hydrogels<sup>5,6</sup>, poly(N,N-dimethylacrylamide) hydrogels<sup>7</sup>, superabsorbent hydrogels<sup>8-11</sup>, graphene-containing stimuli-responsive polymer hydrogels<sup>12,13</sup>, functional hybrid composites<sup>14-18</sup>, amphiphilic hydrogels<sup>19,20</sup>, N-vinylimidazole-based hydrogels<sup>21</sup>, and interpenetrating polymer networks hydrogels<sup>22,23</sup> have been developed by FP. Owing to their unique properties, these hydrogels are widely applied in diverse applications, such as scaffolds for tissue engineering<sup>24,25</sup>, cell-encapsulating devices for drug delivery<sup>26-29</sup>, media for electrophoresis<sup>30,31</sup>, extracellular matrices for biological tissue studies<sup>32-34</sup>, soft contact lenses<sup>35</sup>, actuators and sensors in soft machines<sup>36, 37</sup>, packers in oilfields<sup>38</sup>, and absorbents in waste managements<sup>39,40</sup>.

Recently, Chen *et al.* developed plasma-ignited frontal polymerization for the synthesis of white light-emitting

fluorescent polymer nanocomposites<sup>14, 41</sup> and amphiphilic hydrogels<sup>19,20</sup>, magnetically induced frontal polymerization for constructing robust self-healing host-guest hydrogels<sup>42</sup>, as well as laser-ignited frontal polymerization (LIFP) for the preparation of poly(NMA-*co*-VCL) hydrogels<sup>43</sup> and 4-vinylpyridine-based hydrogels<sup>44</sup>. Among the above methods, laser-ignited frontal polymerization as a new FP model has been demonstrated to treat wastes with remote control and convenience.

In this work, poly(DMAEMA-*co*-AA) hydrogels were successfully synthesized via a simple LIFP route, along with the first investigation of its horizontal direction LIFP. The dependence of the front velocity and front temperature on the AA/DMAEMA molar ratios, initiator concentrations, as well as chemical structures and swelling behaviour of poly(DMAEMA-*co*-AA) hydrogels, were thoroughly investigated in detail. The as-prepared hydrogels are sensitive to pH values ranging from 2 to 12, and their maximum equilibrium swelling ratio could reach 2497 % in pH=7. Horizontal direction LIFP could easily dispose spillings of toxic substances without close contact to the harmful substances, such as the sealing of dye waste liquids through LIFP horizontally. Subsequently, the adsorption of as-prepared hydrogels towards an anionic dye and a cationic dye was also investigated, respectively. The results presented that these hydrogels confer high adsorption performance to dyes through electrostatic interaction.



**Scheme 1** Schematic illustration of the fabrication route to prepare poly(DMAEMA-*co*-AA) hydrogels and application on adsorption

## 2. Experiment

### 2.1 Materials

Dimethylaminoethyl Methacrylate, Acrylic Acid, N-methyl-2-pyrrolidone (NMP), and N,N-methylenebisacrylamide (MBAA) and redox couple, ammonium persulfate (APS)/N,N,N',N'-tetramethylethylenediamine (TMEDA) and dyes orange G (OG) and methylene blue (MB) were all commercially available, at analytical reagent-grade and used without further purification.

### 2.2 LIFP of poly(DMAEMA-*co*-AA) hydrogels

The anionic monomer AA and the cationic monomer DMAEMA were polymerized by LIFP to obtain poly(DMAEMA-*co*-AA) hydrogels (see Scheme 1). Aiming at decreasing the triggering temperature and front temperature, we chose the APS/TMEDA couple as the redox initiator to obtain the transparent hydrogels without bubbles. First of all, the appropriate amounts of DMAEMA and AA were dissolved in NMP in a beaker with the assistance of ultrasound. Then, APS and MBAA were added and shaken vigorously at ambient temperature to obtain a homogeneous mixture. Finally, the homogeneous solution was obtained with mixing the reductant TMEDA and poured into a 10 mL ( $D = 15$  mm) glass test tube. A typical composition was AA/DMAEMA = 8:4 mol/mol, (DMAEMA+AA) = 8 g, NMP = 40 wt %, APS = 0.8 wt%, [APS]/[TMEDA] = 1:4 mol/mol, MBAA = 0.6 wt%. The reaction mixture was kept at ambient temperature to slow down bulk polymerization. Subsequently, infrared laser (C-60) was utilized to irradiate the upper side of the mixture until the formation of a stable front. The whole laser treatment process was 67 s, and the current was kept at 4 mA.

### 2.3 LIFP horizontally of poly(DMAEMA-*co*-AA) hydrogels

In a typical run for the synthesis of poly (DMAEMA-*co*-AA) hydrogels by LIFP horizontally, the appropriate amounts of DMAEMA and AA were dissolved in NMP in a beaker with the assistance of ultrasound. Then, APS and MBAA were added and shaken vigorously at ambient temperature to obtain a homogeneous mixture. Finally, the homogeneous solution was obtained with mixing the reductant TMEDA and poured into a railboat (70 mm $\times$ 1.5 mm) which could be filled with 5 g of monomer mixture. In this case, LIFP horizontally was triggered one end of the railboat vessel by the laser irradiation until a horizontal hot traveling front was formed on the condition of triggering current at 4 mA, while the reaction mixture was kept at ambient temperature (27 °C). The whole laser treatment process remained 45 s. Initial condition: AA/DMAEMA = 8:4 mol/mol, NMP = 40 wt%, MBAA = 0.6 wt%, APS=0.8 wt%, and [APS]/[TMEDA] = 1:4 mol/mol.

### 2.4 Batch polymerization (BP)

Several batch runs were performed in order to compare the resultant samples with the corresponding ones obtained by LIFP. In a typical run, the same amounts of each component as quoted above were mixed with vigorous stirring until homogenization. The final resultant was poured into a reaction vessel and the reaction temperature was set at 60 °C for 2 h.

### 2.5 Velocity and front temperature measurements

The front velocity was confirmed from the slope of line obtained by recording the front position and its corresponding reaction time. A constant front velocity is a strong evidence of occurrence of a pure free-radical FP. Temperature profiles were determined by measuring the temperature as a function of time at a fixed point, using a K-type thermocouple, and then were converted to spatial ones using the front velocities. After the propagating front coming to an end, the end-products were cooled to room temperature and then removed from the vessel for further investigation.

### 2.6 Material characterization

#### 2.6.1 Fourier-transform infrared analysis

To further investigate the chemical structure of the polymeric compound, Fourier-transform infrared (FTIR) analysis was performed using a Nicolet-6700 spectrometer from Thermo Electron at room temperature.

#### 2.6.2 Thermogravimetric analysis

The thermal property of polymeric compound was determined with thermogravimetric apparatus (Shimadzu-TGA 50) in a nitrogen atmosphere with a heating rate of 10 °C/min from 40 to 1000 °C. Samples produced by LIFP were prepared by drying in a vacuum oven at 90 °C for 2 days at a pressure of 70 kPa.

#### 2.6.3 Swelling measurement

The swelling properties of the as-prepared hydrogels were demonstrated by gravimetric analysis. Briefly, the dehydrated samples were immersed in Britton-Robinson (B-R) buffer solution at room temperature. At intervals, the hydrogels were drew out from the medium, weighed after wiping off the excess solution with filter paper, and then taken back to original solution. The measurements were operated again and again until the weight of hydrogels remained stable at a constant value. The swelling ratio (SR, %) was calculated using the following equation:

$$SR = (W_i - W_0) / W_0 \times 100\% \quad (1)$$

Here,  $W_i$  and  $W_0$  are the weights of the swollen and dry hydrogels, respectively.

#### 2.6.4 SEM measurement

The morphology of the resultant samples obtained was investigated by SEM with a QUANTA 200 (Philips-FEI, Holland) at 20.0 kV. The sliced samples were immersed in excess deionized water at room temperature for a week. The water was changed daily to get rid of the water-soluble materials and then the samples were put in a vacuum oven at 60 °C for completely drying. The dried samples were then immersed in solution until they swelled to the extent of maximum. Afterwards, the samples were freeze-dried for 20 h. Treated samples used for SEM measurement were cut to expose their inner structure.

#### 2.6.5 Adsorption equilibrium experiments

The capability for LIFP prepared hydrogels with the different pH values ranged from 2 to 12 adsorbing anionic dye OG and the cationic dye MB was investigated, respectively. The dyes were adsorbed onto the poly(DMAEMA-*co*-AA) in batch experiments, in which 100 mL dye solution with initial concentration of 60 mg/L was taken in a sealed vessel, and 0.10 ( $\pm 0.0050$ ) g of hydrogels was added to it. At intervals, approximately 0.5 mL of the dye solution was removed for analysis at various times. The dye concentration was analysed using a Gold Spectrumlab 54 Ultraviolet-visible (UV-vis) spectrophotometer. Predetermined calibration curves were used to convert the absorbance values at the wavelength corresponding to maximum absorbance ( $\lambda_{\max}$ ) into dye concentrations. All of the experiments were triplicated. The amounts of dye adsorbed on the hydrogel were determined according to the following equation:

$$q_e = (C_o - C_e)V / m \quad (2)$$

Where  $m$  (g) represents the mass of the sample,  $C_o$  and  $C_e$  (mg/L) are the initial and equilibrium dye concentrations, similarly,  $V$  (L) are the volume of solutions.

### 3. Results and discussion

#### 3.1 LIFP of poly(DMAEMA-*co*-AA) hydrogels

Our preliminary experiments aimed to obtain poly(DMAEMA-*co*-AA) hydrogels by LIFP along with a stable front, and to

prohibit occurrence of spontaneous polymerization (SP). Firstly, the pot life of reagents which were put in the container at room temperature until SP occurred. The result shows that the homogeneous reactant mixture was still remain inert in two hours at ambient temperature, while became reactive when was treated for only several seconds with the infrared laser. As described in the schematic of the preparation of poly(DMAEMA-*co*-AA) hydrogels by LIFP, the upper layer of the solution was initiated via infrared laser for about 67 s, whereas the other end of the tube remained open to atmospheric pressure. After initiation, the exothermic nature of polymerizations promotes an increase of temperature at the adjacent portion of the reactor, which triggers the polymerization of the monomers allocated therein.

If the polymerization frontal propagated along the entire reactor at a constant velocity, we can infer the occurrence of pure FP excluding the SP. Fig. 1a shows typical data for the positions of the thermal propagation front as a function of time. The experimental data are well fitted by a straight line, indicating that a constant-velocity, self-sustaining front is achieved. This is a strong proof which reveals no undesired SP takes place; otherwise a simultaneous SP can bring about a deviation from linearity which can be obvious observed in the Fig. 1a. Another key feature to confirm the above judgment is given by the analysis of temperature profile. As shown in Fig. 1b, a horizontal part on the left side of curve mean that temperature is not variable until the front arrived at the fixed point, which is a symbol of pure LIFP without SP. Besides, in less than 0.93 cm, the temperature begins to increase obviously. The tendency of the temperature increasing can be observed by IR thermal imager due to the exothermic reaction, and the  $T_{\max}$  reaches 87 °C.

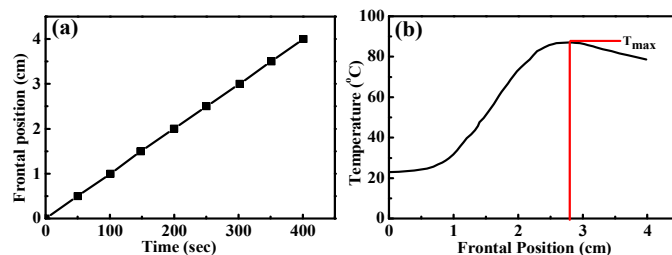


**Fig. 1** (a) Front position versus time for poly(DMAEMA-*co*-AA) hydrogels prepared by LIFP. (b) Typical temperature profile of poly(DMAEMA-*co*-AA) hydrogels prepared by LIFP. Initial condition: AA/DMAEMA=7:3 mol/mol, NMP=40 wt %, APS = 0.8 wt %, [APS]/[TMEDA] = 1:4 mol/mol.

#### 3.2 Effects of AA/DMAEMA molar ratios on LIFP

To investigate effects of AA/DMAEMA molar ratios on the feature of LIFP, a serial of molar ratios of AA to DMAEMA ranging from 6:4 to 9:3 (mol/mol) were run by the method of LIFP for producing poly(DMAEMA-*co*-AA) hydrogels. As shown in Fig. 2a, all the relations between front position and time are perfectly in line with straight lines, which indicate that the propagation of the thermal fronts moved at constant

velocities. Fig. 2b shows  $V_f$  and  $T_{max}$  of poly(DMAEMA-co-AA) as a function of several AA/DMAEMA molar ratios. In terms of the LIFP run, the  $V_f$  at AA/DMAEMA = 6:4, 8:4, 7:3, 9:3 mol/mol are 0.25, 0.38, 0.60, and 0.88 cm/min accordingly. Similar to this velocity trend, increasing the AA/DMAEMA from 6:4 to 9:3 mol/mol induces  $T_{max}$  to range from 65 to 96 °C. From Fig 2b, we can easily conclude that  $T_{max}$  and  $V_f$  both increase as the proportion of AA is elevated. Indeed, at AA/DMAEMA = 9:3 mol/mol, two parameters ( $T_{max}$  and  $V_f$ ) get to the maximum values, respectively, which could be ascribed to the higher reactivity of AA toward radical polymerization. In other words,  $V_f$  and  $T_{max}$  values can be adjusted by regulating the molar ratios of AA/DMAEMA in this system.

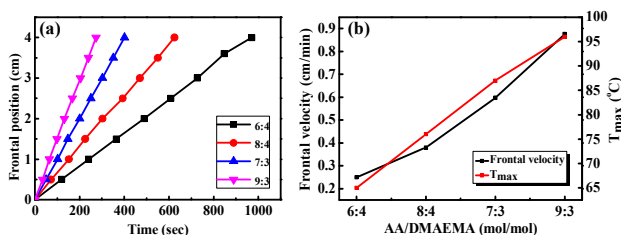


**Fig. 2** (a) Front position versus time of poly(DMAEMA-co-AA) hydrogels prepared by LIFP with different molar ratios of AA/DMAEMA. (b)  $V_f$  and  $T_{max}$  of poly(DMAEMA-co-AA) hydrogels versus molar ratios. Initial conditions: NMP=40 wt %, APS = 0.8 wt %, MBAA = 0.6 wt% and [APS]/[TMEDA] = 1:4 mol/mol.

### 3.3 Effect of the initiator concentration on LIFP

The initiator concentration turns out to be an important factor on LIFP. Generally, under too low initiator concentrations, the front will suspend because of the heat loss. On the contrary, the pot life was too short to achieve FP, which resulted in the heterogeneous polymer finally. In order to optimize initiator concentrations, several runs at different APS concentrations varying from 0.80 wt% to 1.4 wt% with [APS]/[TMEDA]=1:4 mol/mol were performed. We have found that the front can't be propagated in case of APS concentration less than 0.80 wt%, oppositely, many bubbles will occur in the system when APS concentration is more than 1.4 wt%. Therefore, all of the runs were performed for the APS concentrations ranged from 0.8 to 1.4 %. The  $V_f$  and  $T_{max}$  as a function of APS concentration are described in Fig. 3b. As expected, the front velocity monotonically increases from 0.37 to 0.56 cm/min when the initiator concentration is increased gradually. It is observed that  $T_{max}$  can be obviously changed by altering initiator concentrations. Over the entire range of APS concentrations from 0.8 to 1.4 wt%,  $T_{max}$  begins to go up from 76 to 96 °C. The dependence of  $T_{max}$  on the initiator concentration is parallel to the corresponding  $V_f$  trend. Besides, it should be noted that our operation was performed under nonadiabatic condition, so the increased velocity reduced versus the time due to heat loss.

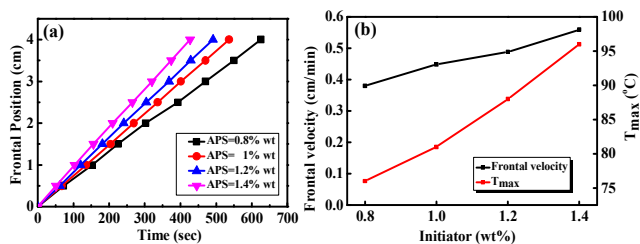


**Fig. 3** (a) Front position versus time of poly(DMAEMA-co-AA) prepared by LIFP at different initiator concentration. (b)  $V_f$  and  $T_{max}$  versus the initiator concentration. Initial conditions: AA/DMAEMA=8:4 mol/mol, NMP = 40 wt%, MBAA = 0.6 wt% and [APS]/[TMEDA] = 1:4 mol/mol.

### 3.4 Swelling behaviour of poly(DMAEMA-co-AA) hydrogels by LIFP

The swelling capability of AA/DMAEMA hydrogels obtained via LIFP in water (pH=7.0) at different molar ratios of AA/DMAEMA was investigated by using gravimetric analysis (Fig. 4). The overall trend is that the SRs of all the samples gradually increase with the swelling time and finally tend to an equilibrium swelling ratio (ESR). As shown in Fig. 4, the swelling ratios of the hydrogels reaches equilibrium states after 80 h, and the ESRs are 2497%, 1427 %, 734 %, and 159 %, corresponding monomer molar ratios of AA/DMAEMA=6:4, 8:4, 7:3, 9:3, respectively. It has been found that higher AA concentration gives rise to lower water SRs. By comparison, BP reaction at the same composition with that of LIFP was performed. As seen in Fig. 4e, the ESR of the sample synthesized by BP is 977%, whereas the ESR of the one obtained by LIFP is 1427%, indicating that the swelling capacity of the hydrogel synthesized via the LIFP is superior to that obtained via the BP.

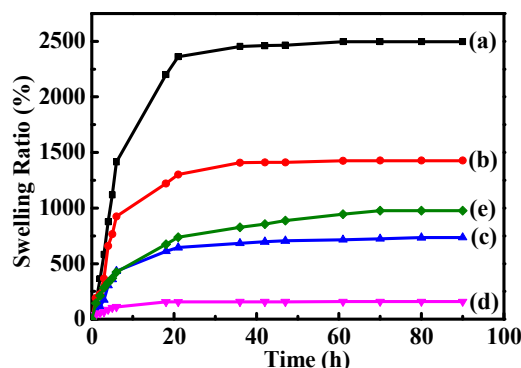


**Fig. 4** Swelling kinetics of poly(DMAEMA-co-AA) hydrogel prepared by LIFP with NMP = 40 wt%, MBAA = 0.6 wt%, APS = 0.8 wt%, and [APS]/[TMEDA] = 1:4 mol/mol at different AA/DMAEMA molar ratios: (a) 6:4, (b) 8:4, (c) 7:3, (d) 9:3 mol/mol. And (e) Swelling kinetics of poly((DMAEMA-co-AA) hydrogel prepared by BP with typical composition.

### 3.5 Characterization of poly(DMAEMA-co-AA) hydrogels

To verify the success of the polymerization, the ATR FT-IR of AA, poly(DMAEMA-co-AA), and DMAEMA were performed,

along with TGA measurement of the resultant polymer. The sliced hydrogels were immersed in deionized water at room temperature for several days to remove residual soluble impurities, daily changing the water during the immersion. Then, the samples were dried in a vacuum oven at 60 °C until the weight of the samples remained constant. Finally, the dried samples were ground into powders for FTIR and TGA characterization. As shown in Fig. 5a curve 1, it can be notably seen that the absorption peaks at 1620 and 1618  $\text{cm}^{-1}$  are assigned to the C=C in DMAEMA and AA segments, disappeared after polymerization. And aliphatic C–N stretching band and the symmetric stretching band of C–O in esters with the C–O–C structure (DMAEMA) are observed at 1384  $\text{cm}^{-1}$  and 1168  $\text{cm}^{-1}$ , respectively. Besides, Fig. 5b is the TGA spectrum of as-prepared hydrogel. There is a single degradation step in the curve, signifying that the as-prepared resultant is a copolymer of AA and DMAEMA; Otherwise, there should be more than one degradation stage in the TGA curve. All results indicate that the copolymerization has occurred and the monomers such as DMAEMA and AA have been incorporated into the resultant hydrogel.

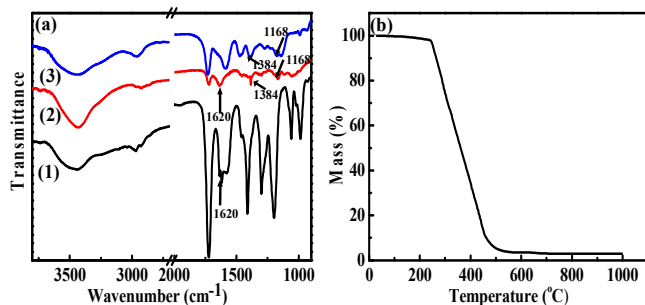


**Fig 5** FTIR spectra recorded at room temperature of (a) (1) AA, (2) DMAEMA and (3) poly(DMAEMA-*co*-AA) (b) TGA curve of poly(DMAEMA-*co*-AA) prepared by LIFP.

### 3.6 Morphology of poly(DMAEMA-*co*-AA) hydrogels

The morphological characteristics of the obtained poly(DMAEMA-*co*-AA) hydrogel with different AA/DMAEMA molar ratios were investigated by SEM. As shown in Fig. 6, the morphological structure of poly(DMAEMA-*co*-AA) hydrogels can distinctly change from spongelike microporous to honeycomb micropore with increasing AA/DMAEMA molar ratios. Specifically, the pore diameters of poly(DMAEMA-*co*-AA) hydrogels at AA/DMAEMA = 6:4, 8:4, 7:3, and 9:3 mol/mol are around 68.30, 46.27, 39.92, and 18.94  $\mu\text{m}$ , respectively, which are in agreement with those of ESR results. That is, the larger pore diameters are and the larger ESR results.

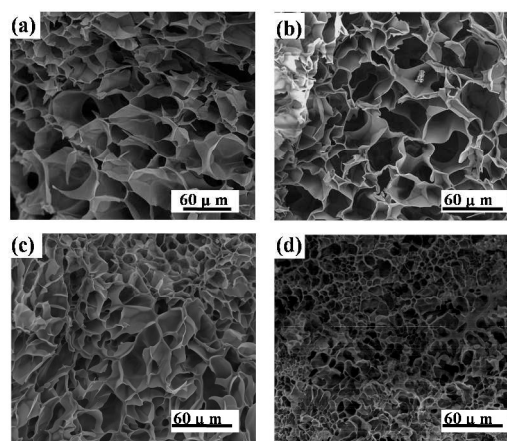


**Fig. 6** SEM micrographs of poly(DMAEMA-*co*-AA) hydrogels prepared by LIFP with MBAA=0.6 wt%, APS=0.8 wt%, [APS]/[TMEDA] =1:4 mol/mol at different AA/DMAEMA molar ratios: (a) 6:4, (b) 8:4, (c) 7:3 and (d) 9:3 (mol/mol).

### 3.7 Swelling capability of poly(DMAEMA-*co*-AA) hydrogels with different pH values

The pH-dependent equilibrium swelling studies were carried out in buffer solutions with pH values ranging from 2 to 12 at room temperature. The swelling equilibrium degrees of hydrogels changing with pH values are shown in Fig. 7. As shown in figure 7a, the swelling degree of all samples increases with the elevated swelling time and finally tend to constant values, namely, ESRs. It has been found that the as-prepared hydrogels are sensitive to pH values. Fig. 7b shows the pH dependence of equilibrium swelling ratio for poly(DMAEMA-*co*-AA) hydrogels. As the pH values of the solution increase from 2 to 6, the poly(DMAEMA-*co*-AA) hydrogels remain in the swollen state; then it exhibits a first-order transition and attains a collapsed state when the pH value of the solution is 6. In the pH range between 6 and 8, the poly(DMAEMA-*co*-AA) hydrogels remain in the collapsed state, while it shows an abrupt swelling above pH= 8. In terms of the resulting structure of the poly(DMAEMA-*co*-AA) hydrogels, the appropriate balance of repulsion and attraction between the carboxyl groups of AA chains and the tertiary amine side groups of DMAEMA chains is assumed to be the key factor for the pH-dependent transition behaviour. In this pH range, the carboxyl–carboxyl and ammonium–ammonium repulsion lead to a high swelling capacity. The attraction between the ammonium and carboxyl groups restricts further swelling, and thus, the swelling capability is highly depended on pH values. These results are consistent with those observed for the swelling capability of an amphoteric polymer, poly(acrylic acid-*co*-diallyldimethyl ammonium chloride)<sup>45</sup> and the swelling capability of an ampholytic polymer, poly(aspartic acid)<sup>46</sup>. Typically, among pH 6–8, the coulombic repulsion and attraction between negative charges of carboxylate anions and the positive charges of ammonium cations are balanced at a level, which result in a collapsed state.

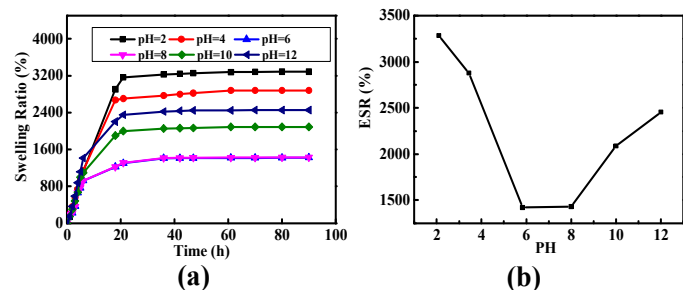


**Fig. 7** (a) Swelling kinetics of poly(DMAEMA-*co*-AA) hydrogels versus different pH values (2, 4, 6, 8, 10, and 12) of medium. (b) pH dependence of equilibrium swelling ratio for poly(DMAEMA-*co*-AA) hydrogels. (AA/DMAEMA = 8:4 mol/mol, NMP = 40 wt%, MBAA = 0.6 wt%, APS = 0.8 wt%, and [APS]/[TMEDA] = 1:4 mol/mol).

### 3.8 LIFP horizontally of poly (DMAEMA-*co*-AA) hydrogels

In order to make the best of LIFP technology, poly (DMAEMA-*co*-AA) hydrogels by LIFP horizontally was investigated. Fig. 8 shows the LIFP process in the horizontal direction. During the entire polymerization process, the temperature variation of fixed point with time could be observed by an IR thermal imager. As shown in Fig. 8a, we can clearly observe hot traveling front moving at a constant velocity. Fig. 8c shows typical data for the position of the thermal propagation front as a function of time. The experimental data are well fitted by a straight line and we figure out the frontal velocity is 1.14 cm/min. This is a strong evidence that pure FP has occurred. Fig. 8b presents the IR thermal images. We can observe that the temperature starts to rise from room temperature, and then gradually increase to the highest point of 82.2 °C in a few minutes. Finally, it has a tendency of dropping slowly. This phenomenon demonstrates another representative feature of pure LIFP. Therefore, we can utilize the LIFP horizontally to treat dye solution effectively, and the resultants are easily peeled off from the vessel without any waste residue. The dye solution was composed of an aqueous solution containing 200 mg/L OG (as shown in Fig. 8d, 8e).

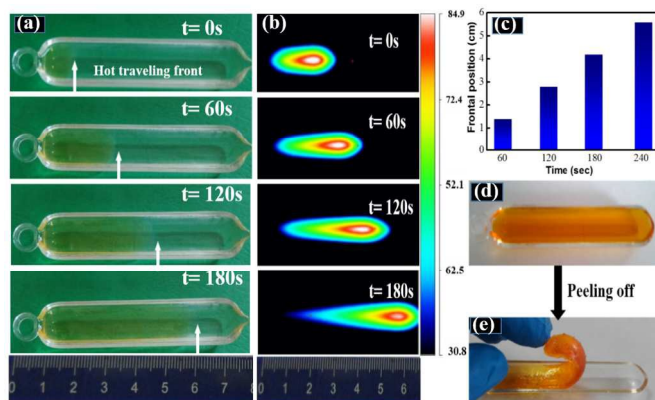


**Fig. 8** (a) Photos of the propagating front of the LIFP horizontally; (b) Corresponding photos took by Fluke Ti30 IR thermal imager; (c)

Front position versus time for hydrogels prepared by LIFP horizontally. (d-e) Dye solution sealing: 200 mg/L OG solution. hydrogels composition: AA/DMAEMA = 8:4 mol/mol, NMP = 40 wt%, MBAA = 0.6 wt%, APS=0.8 wt%, and [APS]/[TMEDA] = 1:4 mol/mol.

### 3.9 Adsorption of poly(DMAEMA-*co*-AA) hydrogels towards dyes under different pH values

We further investigated the adsorption capabilities of poly(DMAEMA-*co*-AA) hydrogels containing carboxyl/amino segments towards MB and OG dyes under different pH values ranging from 2 to 12. The hydrogels with the same composition were employed in all runs with different pH values. After the hydrogels absorbed dyes, the reduction in the concentration of MB and OG with time is shown in Fig. 9a, 9b, respectively. Furthermore, the dye adsorption capacity of hydrogels under different pH values is clearly indicated by Fig. 9c. After hydrogels immersing in dye-loaded B-R buffer solutions at pH = 2, 4, 6, 8, 10, and 12 for about 90 hours, the adsorption capacities of hydrogels for MB are determined to be 7.92, 11.92, 13.01, 45.16, 51.08, 55.03 mg/g, respectively. Likewise, the adsorption capacities of hydrogels for OG are 53.53, 51.02, 50.01, 36.04, 32.42 and 15.31 mg/g, respectively. By comparing the adsorption capacities of hydrogels under acid medium with those under the base medium, it is evident that there is no notable difference for the hydrogel adsorption capacities towards MB dye when pH values range between 2 and 6, revealing that acid medium could not remarkably affect the hydrogel adsorption capacities towards MB. However, the hydrogel adsorption capacities towards MB are highly enhanced when pH values range between 8 and 12. The reason could be explained by that the acid medium allows the hydrogels containing amino segments to be protonated and MB is a cationic dye. This causes a strong electrostatic repulsions between the hydrogels and cationic MB dye. On the contrary, the alkaline environment favours the absorption of MB dye due to the electrostatic attraction. Similarly, Fig. 9b indicates that the hydrogels absorb more OG dye under acid medium since OG is a typical anionic dye.

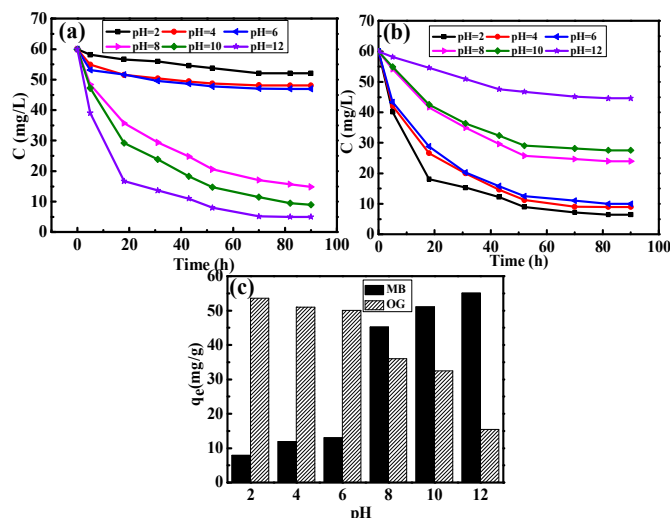


**Fig. 9** Variations in the concentrations of (a) MB and (b) OG with time at different pH values for poly(DMAEMA-co-AA) with AA/DMAEMA = 8:4 mol/mol. (c) The adsorption capacities of poly(DMAEMA-co-AA) hydrogels for MB(left) and OG(right) in solutions of pH = 2, 4, 6, 8, 10, 12.

#### 4. Conclusions

In this work, a series of poly(DMAEMA-co-AA) hydrogels were facilely produced by laser ignited frontal polymerization (LIFP). More importantly, the hydrogels were firstly synthesized by using horizontal LIFP model, which presents horizontal LIFP model confers several advantages, such as rapid synthesis away from the dangerous sites, easily sealing toxic wastes. The effect parameters of frontal polymerization for the as-prepared hydrogels, such as molar ratios of AA/DMAEMA and APS concentrations were thoroughly investigated. The as-prepared hydrogels are sensitive to pH values ranged from 2 to 12, and their maximum equilibrium swelling ratio could reach 2497 % in pH=7. Swelling studies show that the SRs of the poly(DMAEMA-co-AA) hydrogels produced via LIFP are superior to those obtained by BP. Also, the as-prepared hydrogels could effectively absorb MB and OG dyes, which undergo in base medium and acid medium, respectively. That is, they would provide the potential as dye water waste scavenger. In addition, LIFP horizontally was employed to seal dyestuff solutions. This model would expand the scope of LIFP applications on spilled toxic substances without touching the location of the reaction, even on radiation danger zone.

#### Acknowledgements

This work was supported by the National High Technology Research and Development Program of China (863 Program) (2012AA030313), National Natural Science Foundation of China (21006046 and 21474052), Natural Science Foundation of Jiangsu Province (BK20131408), and Priority Academic Program Development of Jiangsu Higher Education Institutions (PAPD).

#### Notes and references

State Key Laboratory of Materials-Oriented Chemical Engineering, and College of Chemistry and Chemical Engineering, Nanjing Tech

University (former: Nanjing University of Technology), Nanjing 210009, P. R. China.

E-mail: chensu@njtech.edu.cn; Fax: 86-25-83172258;

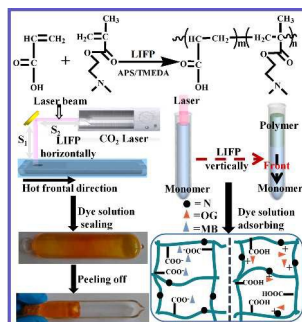
- N. M. Chechilo, R. JKhvilivitskii and N. S. Enikolopyan, *Dokl Akad Nauk SSSR*, 1972, **204**, 1180-1181.
- R. P. Washington and O. Steinbock, *J Am Chem Soc*, 2001, **123**, 7933-7934.
- Q.-Z. Yan, W.-F. Zhang, G.-D. Lu, X.-T. Su and C.-C. Ge, *Chemistry*, 2005, **11**, 6609-6615.
- Q.-Z. Yan, W.-F. Zhang, G.-D. Lu, X.-T. Su and C.-C. Ge, *Chemistry*, 2006, **12**, 3303-3309.
- L. Chen, T. Hu, H. Yu, S. Chen, and J. A. Pojman, *J. Polym. Sci. Part A: Polym. Chem.*, 2007, **45**, 4322-4330.
- J. A. Pojman, G. Curtis, and V. M. Ilyashenko, *J. Am. Chem. Soc.*, 1996, **118**, 3783-3784.
- G. Caria, V. Alzari, O. Monticelli, D. Nuvoli, J. M. Kenny and A. Mariani, *J. Polym. Sci. Part A: Polym. Chem.*, 2009, **47**, 1422-1428.
- H. Shao, C.-F. Wang, S. Chen and C. Xu, *J. Polym. Sci. Part A: Polym. Chem.*, 2014, **52**, 912-920.
- R. B. Zhang, Z. Qiu, H. Qiu and X. Zhang, *J. Appl. Polym. Sci.*, 2014, **131**.
- S. Scognamillo, V. Alzari, D. Nuvoli and A. Mariani, *J. Polym. Sci. Part A: Polym. Chem.*, 2010, **48**, 2486-2490.
- S. Scognamillo, V. Alzari, D. Nuvoli, J. Illescas, S. Marceddu and A. Mariani, *J. Polym. Sci. Part A: Polym. Chem.*, 2011, **49**, 1228-1234.
- V. Alzari, A. Mariani, O. Monticelli, L. Valentini, D. Nuvoli, M. Piccinini, S. Scognamillo, S. B. Bon and J. Illescas, *J. Polym. Sci. Part A: Polym. Chem.*, 2010, **48**, 5375-5381.
- R. Sanna, D. Sanna, V. Alzari, D. Nuvoli, S. Scognamillo, M. Piccinini, M. Lazzari, E. Gioffredi, G. Malucelli and A. Mariani, *J. Polym. Sci. Part A: Polym. Chem.*, 2012, **50**, 4110-4118.
- J. Zhou, H. Shao, J. Tu, Y. Fang, X. Guo, C.-F. Wang, L. Chen and S. Chen, *Chem. Mater.*, 2010, **22**, 5653-5659.
- B. Falk, M. R. Zonca, Jr. and J. V. Crivello, *Macromolecular Symposia*, 2005, **226**, 97-108.
- J. V. Crivello, B. Falk, M. R. Zonca, and JR., *J. Polym. Sci. Part A: Polym. Chem.*, 2004, **42**, 1630-1646.
- S. Chen, J. Sui, L. Chen and J. A. Pojman, *J. Polym. Sci. Part A: Polym. Chem.*, 2005, **43**, 1670-1680.
- I. P. Nagy, L. Sike and J. A. Pojman, *J. Am. Chem. Soc.*, 1995, **117**, 3611-3612.
- J. Tu, L. Chen, Y. Fang, C. Wang and S. Chen, *J. Polym. Sci. Part A: Polym. Chem.*, 2010, **48**, 823-831.
- C. Yu, J. Zhou, C. Wang, L. Chen and S. Chen, *J. Polym. Sci. Part A: Polym. Chem.*, 2011, **49**, 5217-5226.
- J. Tu, J. Zhou, C.-F. Wang, Q. Zhang and S. Chen, *J. Polym. Sci. Part A: Polym. Chem.*, 2010, **48**, 4005-4012.
- J. A. Pojman, W. Elcan, A. M. Khan and L. Mathias, *J. Polym. Sci. Part A: Polym. Chem.*, 1997, **35**, 227-230.
- N. Liu, H. Shao, C.-F. Wang, Q.-L. Chen and S. Chen, *Colloid Polym Sci.*, 2013, **291**, 1871-1879.
- B. Balakrishnan and R. Banerjee, *Chem. Rev.*, 2011, **111**, 4453-4474.
- C. M. Valmikinathan, V. J. Mukhatyar, A. Jain, L. Karumbaiah, M. Dasari and R. V. Bellamkonda, *Soft Matter*, 2012, **8**, 1964.
- Y. Jiang, J. Chen, C. Deng, E. J. Suuronen and Z. Zhong, *Biomaterials.*, 2014, **35**, 4969-4985.
- E. Gavini, A. Mariani, G. Rassu, S. Bidali, G. Spada, M. C. Bonferoni and P. Giunchedi, *Eur Polym J.*, 2009, **45**, 690-699.
- Q. Feng, F. Li, Q.-Z. Yan, Y.-C. Zhu and C.-C. Ge, *Colloid Polym Sci.*, 2010, **288**, 915-921.
- J. J. Schmidt, J. Rowley and H. J. Kong, *J Biomed Mater Res A*, 2008, **87**, 1113-1122.
- M. P. Patel, S. T. Churchman, A. T. Cruchley, M. Braden and D. M. Williams, *Dent. Mater.*, 2013, **29**, 299-307.
- F. Li, S. A. Allison and R. J. Hill, *J Colloid Interface Sci*, 2014, **423**, 129-142.
- B. M. Gillette, J. A. Jensen, M. Wang, J. Tchao and S. K. Sia, *Adv. Mater.*, 2010, **22**, 686-691.
- J. Zhu, J. A. Beamish, C. Tang, K. Kottke-Marchant and R. E. Marchant, *Macromolecules*, 2006, **39**, 1305-1307.

## ARTICLE

- 34 J. Torgersen, X.-H. Qin, Z. Li, A. Ovsianikov, R. Liska and J. Stampfl, *Adv. Funct. Mater.*, 2013, **23**, 4542-4554.
- 35 J. Kopecek, *J. Polym. Sci. Part A: Polym. Chem.*, 2009, **47**, 5929-5946.
- 36 S. Cai, Y. Lou, P. Ganguly, A. Robisson and Z. Suo, *J. Appl. Phys.*, 2010, **107**, 103535.
- 37 N. Gill, J. A. Pojman, J. Willis and J. B. Whitehead, *J. Polym. Sci. Part A: Polym. Chem.*, 2003, **41**, 204-212.
- 38 T. Murosaki, T. Noguchi, K. Hashimoto, A. Kakugo, T. Kurokawa, J. Saito, Y. M. Chen, H. Furukawa and J. P. Gong, *Biofouling*, 2009, **25**, 657-666.
- 39 A. Atta, H. S. Ismail and A. M. Elsaad, *J. Appl. Polym. Sci.*, 2012, **123**, 2500-2510.
- 40 B. Adhikari, G. Palui and A. Banerjee, *Soft Matter*, 2009, **5**, 3452.
- 41 J. Zhou, W.-Q. Tang, C.-F. W, L. Chen, Q. Chen, and S. Chen, *J. Polym. Sci. Part A: Polym. Chem.*, 2012, **50**, 3736-3742.
- 42 C. Yu, C.-F. Wang and S. Chen, *Adv. Funct. Mater.*, 2014, **24**, 1235-1242.
- 43 Z.-F. Zhou, C. Yu, X.-Q. Wang, W.-Q. Tang, C.-F. Wang and S. Chen, *J. Mater. Chem.A*, 2013, **1**, 7326.
- 44 W.-Q. Tang, L.-H. Mao, Z.-F. Zhou, C.-F. Wang, Q.-L. Chen and S. Chen, *Colloid Polym Sci.*, 2014, **292**, 2529-2537.
- 45 S. Xu, R. Wu, X. Huang, L. Cao and J. Wang, *J. Appl. Polym. Sci.*, 2006, **102**, 986-991.
- 46 Y. Zhao, H. Su, L. Fang and T. Tan, *Polymer*, 2005, **46**, 5368-5376

# Facile Access to Poly(DMAEMA-co-AA) Hydrogels via Infrared Laser-Ignited Frontal Polymerization and Its Polymerization in Horizontal Direction

Yan Liu, Cai-Feng Wang, Su Chen\*



pH sensitive hydrogels are fabricated via infrared laser-ignited frontal polymerization (LIFP) and its LIFP in horizontal direction towards dye adsorption.